LBL-19806
c.2

Lawrence Berkeley Laboratory
UNIVERSITY OF CALIFORNIA

DOCUMENTS SECTION

Invited talk presented at the
Conference on Nuclear Structure
with Heavy Ions, Legnaro (Padova), Italy,
May 27-31, 1985

COMPOUND NUCLEUS STUDIES WITH REVERSE KINEMATICS

L.G. Moretto

June 1985

TWO-WEEK LOAN COPY
This is a Library Circulating Copy
which may be borrowed for two weeks.

NUCLEAR SCIENCE DIVISION

LBL-19806
c.2

Prepared for the U.S. Department of Energy under Contract DE-AC03-76SF00098

DISCLAIMER

This document was prepared as an account of work sponsored by the United States Government. While this document is believed to contain correct information, neither the United States Government nor any agency thereof, nor the Regents of the University of California, nor any of their employees, makes any warranty, express or implied, or assumes any legal responsibility for the accuracy, completeness, or usefulness of any information, apparatus, product, or process disclosed, or represents that its use would not infringe privately owned rights. Reference herein to any specific commercial product, process, or service by its trade name, trademark, manufacturer, or otherwise, does not necessarily constitute or imply its endorsement, recommendation, or favoring by the United States Government or any agency thereof, or the Regents of the University of California. The views and opinions of authors expressed herein do not necessarily state or reflect those of the United States Government or any agency thereof or the Regents of the University of California.

LBL-19806

Compound Nucleus Studies with Reverse Kinematics

L.G. Moretto

Nuclear Science Division
Lawrence Berkeley Laboratory
University of California
Berkeley, California 94720

Invited talk, to be published in the Proceedings, Conference on Nuclear Structure with Heavy Ions, Legnaro (Padova), Italy, May 27-31, 1985

This work was supported by the Director, Office of Energy Research, Division of Nuclear Physics of the Office of High Energy and Nuclear Physics of the U.S. Department of Energy under Contract DE-AC03-76SF00098.

Compound Nucleus Studies with Reverse Kinematics

L.G. Moretto

Nuclear Science Division, Lawrence Berkeley Laboratory
University of California, Berkeley, California 94720

Abstract: Reverse kinematics reactions are used to demonstrate the compound nucleus origin of intermediate mass particles at low energies and the extension of the same mechanism at higher energies. No evidence has appeared in our energy range for liquid-vapor equilibrium or cold fragmentation mechanisms.

In this talk I want to show how some existing puzzles in the high energy emissions of nuclei of intermediate mass and charge have led us to the characterization of a low energy compound nucleus mechanism on one hand and to the study and understanding of its high energy counterpart on the other. In the process of developing this research we have amply benefited from a method that, if not essential to the success of our enterprise, has been determinant to the technology of the experiment and to its immediate qualitative understanding. I am speaking of the method of reverse kinematics. I am sure that myself and my experimental colleagues would very much enjoy talking about the relative merits and difficulties of preparing targets of exotic elements or of making the same into beams. From my part I am sure that, at Berkeley, the latter rather than the former solution is the cheapest and the most easily achieved. I have also little doubt that we would delight in the intriguing possibilities of eliminating the damaging effects of target contamination with reverse kinematics, not to speak of bringing rare events out of the mud of background into the crisp air of a noiseless environment. However, out of respect for our theoretical colleagues who delight in different preciosities, let us go back to physics, having, in my mind, amply justified the title, as the excuse it is for telling you some of our recent work.

Complex particles have appeared very early and obscurely in the game of nuclear physics, ever since radiochemists bombarded a variety of targets with high energy protons and managed to fish out of the resulting soup a few light radioactive elements.[1] The same particles made their debut in the society of instrumental nuclear physics when they were detected by means of particle telescopes in the reaction of U, Ag with GeV protons,[2] although nobody paid much attention to them either. Recently a new interest, probably stirred by the abundance of their production in heavy ion reactions, has brought these particles in the limelight. We have all heard of at least two interpretations regarding their origin. The first claims these particles to be the result of nuclear shattering or cold fragmentation.[3] The second sees them produced as droplets condensing out of a vapor at or near the critical temperature.[4] Things being confused as they were, at least to me, I felt it would be worth trying to clarify the picture by going way down in energy and in particular by checking whether the compound nucleus itself could not be one of their possible sources through a mechanism somehow intermediate between standard evaporation and fission.

In fact the experimental distinction between the processes of evaporation and fission in relatively heavy compound nuclei can be understood in terms of a specific topological feature in the liquid drop model potential

energy surface V(Z) as a function of mass asymmetry Z. This feature is a deep minimum at symmetry (fission region) flanked at greater asymmetries by the Businaro-Gallone mountains which in turn descend at even larger asymmetries ("evaporation" region). The corresponding mass distribution expected for compound nucleus decay is approximately proportional to $\exp[-V(Z)/T_Z]$, where T_Z is the temperature of the conditional saddle point, and indeed shows a peak at symmetry (fission peak) and two wings at the extreme asymmetries (evaporation wings).

In progressively lighter compound nuclei the potential energy surface undergoes a topological change as the fissionability parameter x crosses the Businaro-Gallone point. At this point the second derivative of the potential energy with respect to the mass asymmetry coordinate evaluated at symmetry vanishes. Thus below the Businaro-Gallone point there is no longer a true fission saddle point, and the monotonically increasing potential energy towards symmetry determines the disappearance of fission as a process distinct from evaporation. In other words the mass distribution should show the two evaporation wings extending as far as symmetry where a minimum should be observed. These features are illustrated in fig. 1.

Within this framework, it has been possible to describe, in a continuous way, the transition from light particle emission to fission.[5] This theory also predicts changes in the shapes of both the kinetic energy spectra and angular distributions of the emitted fragments as their masses increase from α-particles toward fission fragments. These predictions[5] are amenable to experimental test; unfortunately, there is a surprising lack of experimental data that can be compared with the above unified treatments or with more standard formalisms.

We have obtained experimental evidence for the emission of complex nuclei from helium through fluorine by compound nuclei produced in the reaction 90 MeV ^{3}He + ^{nat}Ag.[6] The specific choice of ^{3}He as projectile was dictated by two reasons. On one hand it is desirable to have a relatively low velocity projectile in order to minimize pre-equilibrium losses, but massive enough to bring in sufficient energy. On the other, the mass of the projectile should be sufficiently smaller than those of the complex fragments of interest in order to rule out the ambiguity of projectile fragmentation or multinucleon transfer.

In order to determine the existence of an isotropically emitting source and its velocity, the laboratory energy spectra were transformed into invariant cross-section plots in velocity space which are presented in Fig. 2. The peak cross section for a heavy complex fragment, such as carbon, has a constant value and occurs at the same c.m. velocity from 170° to 40° (as indicated by the position of the X's relative to the circular arc). At the most forward angle the peak cross section occurs at a slightly increased velocity. Similarly, the higher velocity region (the region near the arc with the larger radius) shows no significant change in the backward hemisphere, but does stretch out at forward angles. For a light complex fragment such as Li, the peak of the cross section occurs at a constant c.m. velocity for a smaller backward angle region (170° to 120°). Forward of 120° the peak increases both in cross section and in velocity. The slope of the high-energy tail does not change significantly for the three most backward angles, but the intensity of the tail increases as the scattering angle decreases. The ^{9}Be and B fragments show a behavior intermediate between that of Li and C. In general, the heavier ejectiles show patterns more consistent with the emission from a single source.

Two conclusions can be drawn from these invariant cross-section plots. First, for all elements there is an angular region in the backward hemisphere where only a single component is observed, which can be charac-

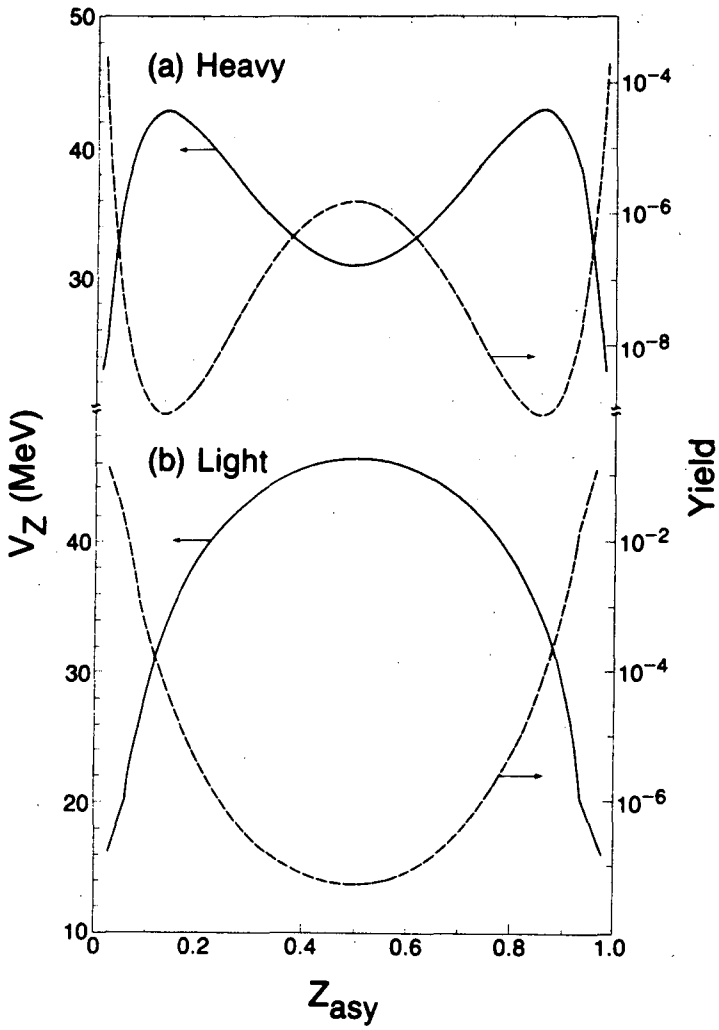

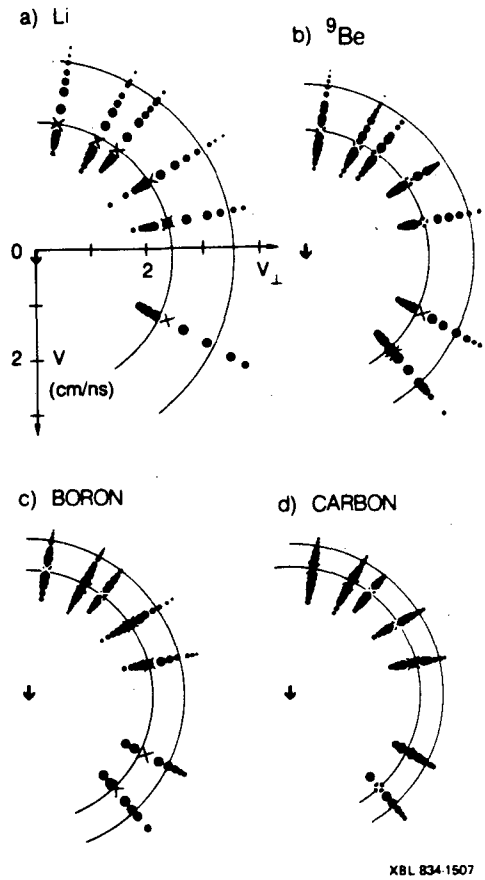

Fig. 1. Comparison of the potential energy surfaces (solid curve) and expected yields (dashed curve) for a) a heavy CN (Au at $\ell = 0$ and $E^* = 97$ MeV) and b) a light CN (Ge at $\ell = 0$ and $E^* = 72$ MeV).

Fig. 2. Invariant cross section plots $\left(\propto \frac{1}{V^2}\frac{d^2\sigma}{d\Omega dV}\right)$ for representative ejectiles (Li, ^{9}Be, B, and C). The diameter of the dots is proportional to the logarithm of the cross section and the X's indicate the peak of velocity distribution. The two large arcs are sections of circles centered on the c.m. velocity (center arrow) appropriate for complete fusion. The beam direction (0°) is indicated by the c.m. velocity vector.

terized as c.m. emission. This angular region increases and extends to more forward angles as the ejectile mass increases. Second, there is a component of non-c.m. emission that results in harder energy (or velocity) spectra at forward angles.

The energy spectra of the equilibrium component in the c.m. system are shown in Fig. 3. The mean energies of the spectra are Coulomb-like and increase as the charge of the fragment increases. The most interesting feature in the energy spectra of the equilibrium component is the evolution from a Maxwellian shape for α-particles (not shown) or Li ions through a more symmetric shape for B or C to a symmetric shape for the heaviest ejectiles, as predicted in Ref. 5. In previous high energy proton studies,[7-8] an exponential tail was observed for all ejectiles. This tail, produced by sources other than equilibrium emission from the center-of-mass system, masks the shape of the equilibrium component. At forward angles, our data also show the presence of a nonequilibrium exponential tail.

The experimental yields of the equilibrium component are shown in Fig. 4. In order to minimize contributions from sources other than the compound nucleus, we have plotted the yields only for the most backward angle (171°). These yields drop precipitously in going from Z = 2 to Z = 3, after which they decrease more slowly. The one exception is the enhanced Z = 6 yield.

The yield from an equilibrium statistical emission process should be roughly proportional to a factor $\exp[-B_Z/T_Z]$, where B_Z is the emission barrier for fragment Z and T_Z is the temperature at the barrier. More quantitatively, the decay width is given by

$$\Gamma_Z \propto T_Z[E/(E - B_Z)]^2 \exp[2\sqrt{a(E - B_Z)} - 2\sqrt{aE}] \tag{1}$$

$$\tilde{\propto} \exp[-B_Z/T_Z] \quad . \tag{2}$$

To calculate the theoretical yields, the following expression for the barrier was used

$$B_Z = U_1 + U_2 + \frac{Z_1 Z_2 e^2}{d} + U_{prox} - U_{CN} \quad , \tag{3}$$

where U_1 is the experimental mass of the light fragment, U_2, U_{CN} are the droplet model masses of the residual and compound nucleus, respectively, and U_{prox} is the proximity potential. The center-to-center distance d in the interfragment Coulomb term was taken to be $d = 1.225(A_1^{1/3} + A_2^{1/3}) + 2$ fm. The addition of 2 fm was done to obtain rough agreement with the energy spectra. The temperature (T_Z) was evaluated using $E - B_Z = aT_Z^2$. A compound nucleus excitation energy (E) of 102 MeV (the value for full momentum transfer) and a level density parameter (a) of A/8 were assumed. The calculated yields (Eq. 1) for each isotope were multiplied by 2I + 1 (where I is the ground state spin of the light fragment) and then summed. The theoretical ejectile yields were calculated as a ratio Γ_Z/Γ_6 and have been normalized to the data at Z = 6 in Fig. 4.

The agreement between the data (circles) and this simple equilibrium statistical calculation (solid line) is exceptionally good for Z = 3-9. The calculation underpredicts the α-particle yield because it only takes into account first chance emission, whereas substantial amounts of higher chance α-emission occur. Precompound emission is expected to leave the compound nucleus with a broad excitation energy distribution with a most probable value of ~85 MeV. A calculation (not shown) with this lower excitation energy also reproduces the relative yields of the heavy fragments quite well but overpredicts the yield of first chance α-emission. More detailed com-

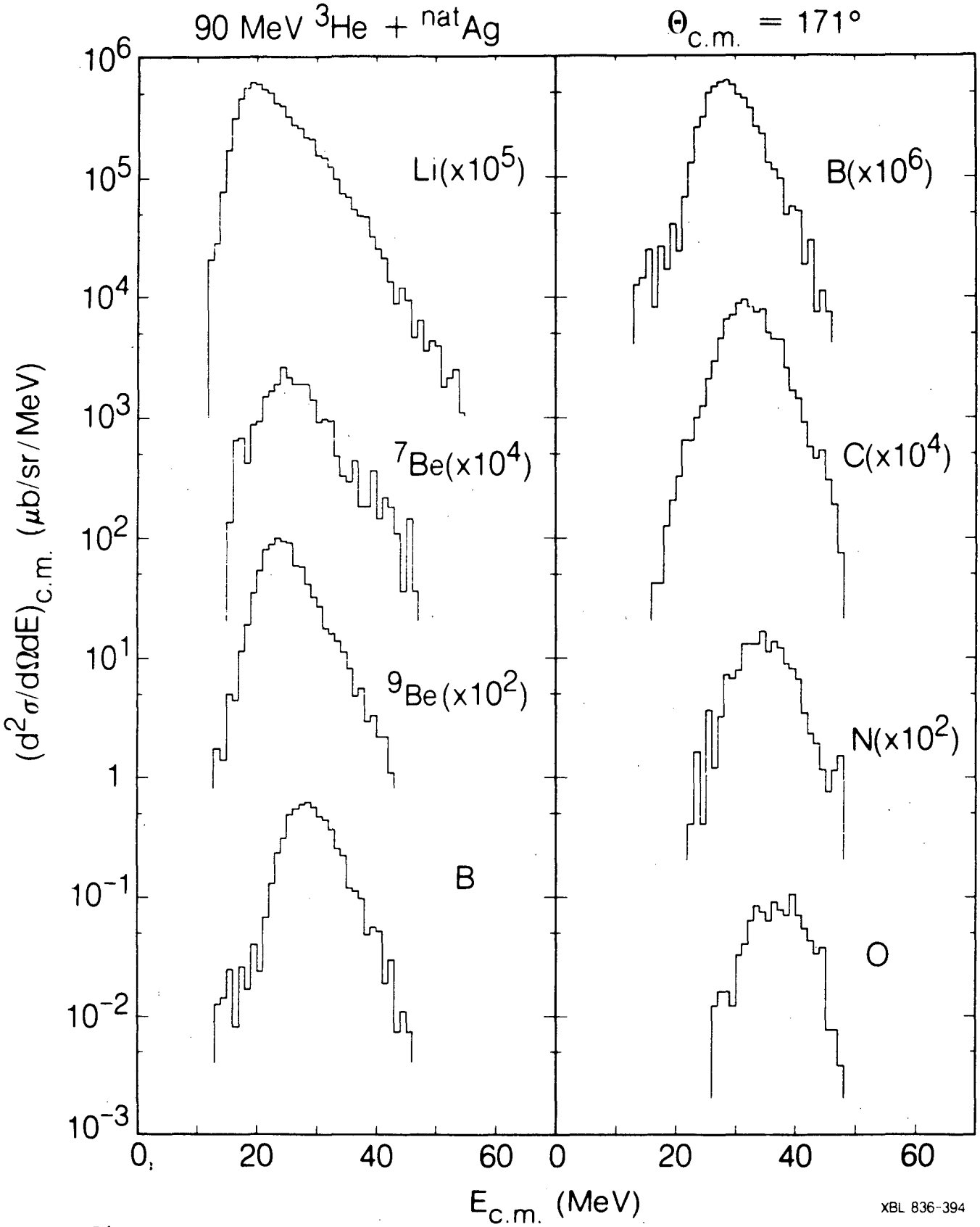

Fig. 3. Energy spectra in the c.m. system for various ejectiles detected at $\theta_{c.m.}$ = 171°. Before correction for carbon contamination the lower level threshold varied from 4 to 12 MeV in the c.m.for Li to O ejectiles, respectively.

parisons between the data and theory require calculations that include precompound emission; however, the substantial agreement depicted in Fig. 4 does indicate that an equilibrated process is responsible for the emission of these complex fragments.

Complete excitation functions obtained from the $^{3}He + {}^{nat}Ag$ measurements are shown in Fig. 5 for a series of decay products. The measurements were restricted to the backward angles (120° - 160°) in order to insure measurement of only the equilibrium component.

With increasing bombarding energy, the cross sections (see Fig. 5) rise rapidly and then flatten at higher energies. This is a characteristic signature of compound nucleus emission, and reinforces the assignment of compound nucleus decay that was made previously on the basis of data obtained at 90 MeV. The cross section for Z = 3 is a factor of 1000 lower than that for Z = 2, and for the heavier fragments it is even lower. In spite of these low cross sections, we were able to measure an excitation function over 2-3 orders of magnitude up to Z = 11, with a detection limit of about 50 nb.

The experimental excitation function data have been fitted using a transition state formalism, analogous to that used to fit fission excitation functions.[5] As shown in Ref. 5, the decay width for first-chance emission of a fragment of charge Z can be written as

$$\Gamma_Z = \frac{1}{2\pi\rho(E)} \int_0^{E-B_Z} \rho_Z^*(E - B_Z - \varepsilon)d\varepsilon \tag{4}$$

where $\rho(E)$ is the compound nucleus level density, B_Z is the conditional barrier height, and $\rho_Z^*(E - B_Z - \varepsilon)$ is the level density at the conditional saddle with a kinetic energy ε in the decay mode. The neutron width Γ_n can be written as

$$\Gamma_n = \frac{2mR^2g}{2\pi\rho(E)} \int_0^{E-B_n} \varepsilon\rho(E - B_n - \varepsilon)d\varepsilon \tag{5}$$

We make the assumption that the ratio of the decay widths, Γ_Z/Γ_n, is proportional to the ratio of the cross section for complex fragment emission, σ_Z, to that for complete fusion, σ_f, i.e.,

$$\Gamma_Z/\Gamma_n \simeq \frac{\Gamma_Z}{\Gamma_t} \simeq \frac{\sigma_Z}{\sigma_t} \simeq \frac{\sigma_Z}{\sigma_R} \tag{6}$$

This is reasonable in this mass region because $\Gamma_n \gg \sum_{Z\geq 1}^{\infty} \Gamma_Z$. One can then calculate $\Gamma_Z/\Gamma_n(E)$ using an appropriate choice for the level density expression. A Fermi gas level was used because it gives an analytical expression for Γ_Z/Γ_n. A simple angular momentum dependence has been included by adding to the barriers the rotational energies appropriate to the ground and saddle point deformations.

Using the above expression for Γ_Z/Γ_n, the barriers B_Z, and the ratio a_Z/a_n, of the level density parameters were extracted from fits to the experimental data σ_Z/σ_R. These fits are shown by the solid lines in Fig. 5. The agreement between the data and the fits is remarkably good for all Z-values and confirms that these products originate from compound nuclear decay.

The barriers extracted from the fits are shown by the circles in Fig. 6 as a function of Z. The extracted barriers increase dramatically as the

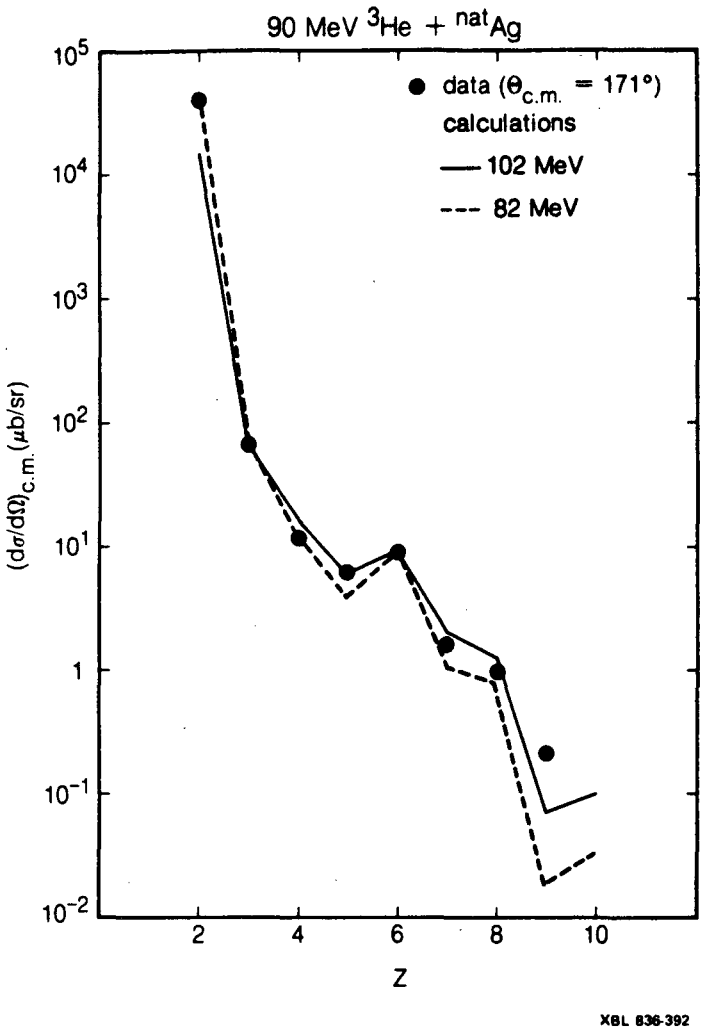

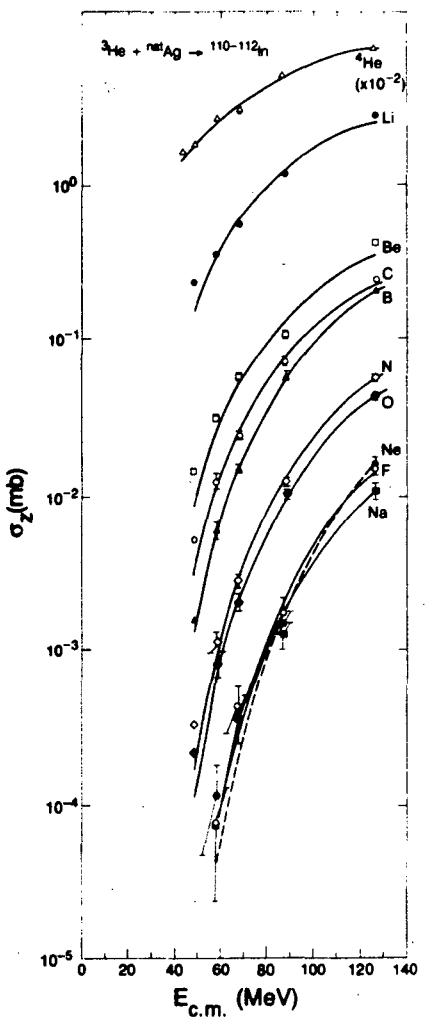

Fig. 4. Experimental (circles) and theoretical yields versus ejectile atomic number (Z).

Fig. 5. Dependence of the total integrated cross sections for emission of complex fragments on the center-of-mass energy, $E_{c.m.}$ in the reaction ^{3}He + ^{nat}Ag. The points and error bars correspond to the experimental cross sections. The curves are fits with the parameters of Fig. 6.

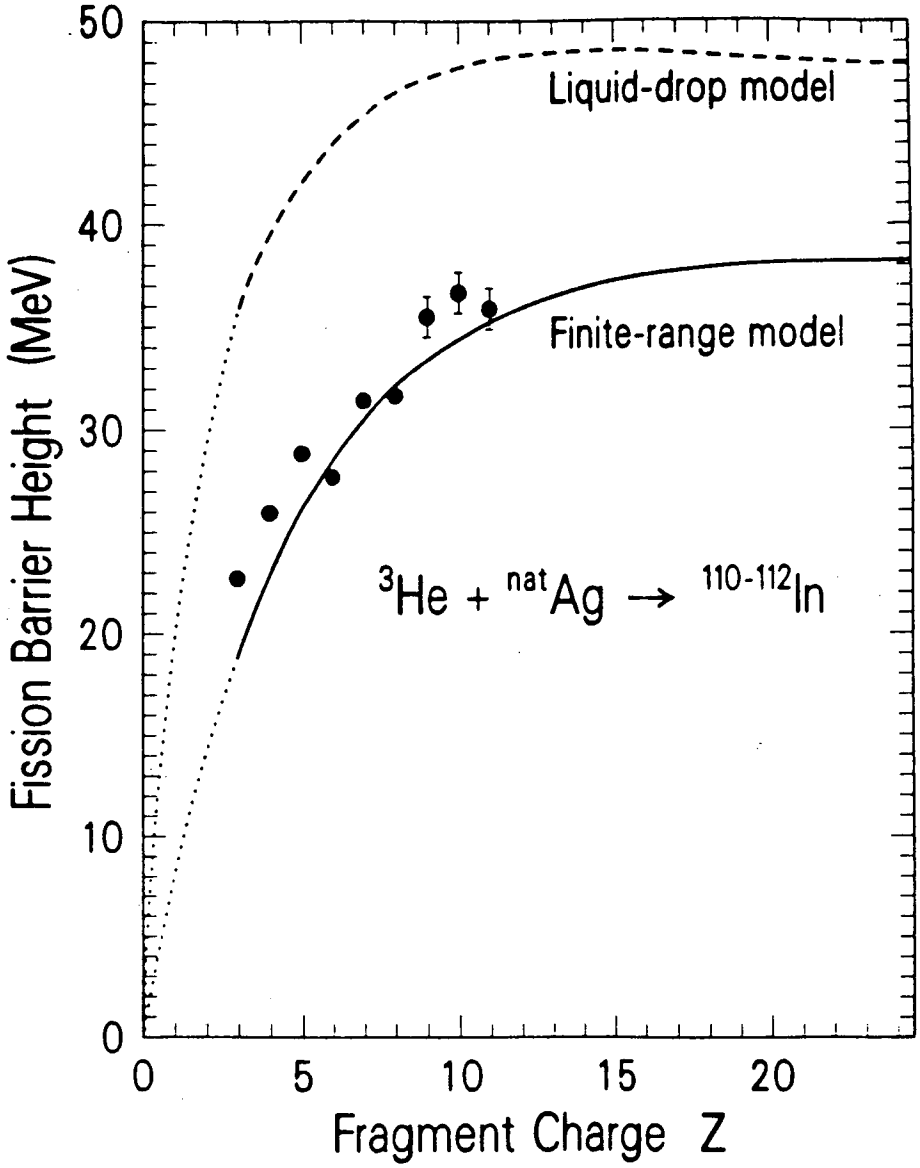

Fig. 6. The emission barriers, B_Z, extracted in fitting the excitation emission of complex fragments functions as a function of fragment charge. The liquid drop model and finite range model calculations are from ref. 9.

exit channel becomes more symmetric. Some evidence of shell effects in the exit channel is visible in the barrier for carbon emission, Z = 6, which is lower than those of the neighboring elements.

The barriers so obtained can be used to test modern corrections to the liquid drop model, like surface diffuseness and finite range, which become important for strongly indented saddle configurations like those presiding to the emission of complex fragments. A comparison of the standard liquid drop model prediction and of the model incorporating the corrections mentioned above[9] with our data is also shown in fig. 6. Clearly our data strongly support the introduction of surface diffuseness and finite range. It is also easy to understand how these and similar data may be very valuable in fixing the relevant parameters of the model.

As mentioned before, the sharp distinction between evaporation and fis-

sion in relatively heavy compound nuclei is a result of a specific topological feature of the liquid drop model potential energy surface V(Z) as a function of mass asymmetry Z. The potential energy shows a deep minimum at symmetry (fission region) surrounded by the Businaro-Gallone mountains which in turn descend at even larger asymmetries ("evaporation" region). The corresponding mass distribution from compound nucleus decay shows a peak at symmetry (fission peak) and two wings at the extreme asymmetries (evaporation wings). The qualitative dependence of the potential energy and of the mass yield vs. asymmetry is shown in Fig. 1a for a heavy nucleus.

With decreasing total mass the potential energy surface undergoes a qualitative change when the fissility parameter x crosses the so-called Businaro-Gallone point. At this point (x_{BG} = 0.396 for ℓ = 0 and decreasing for larger ℓ values) the second derivative of the potential energy with respect to the mass asymmetry coordinate evaluated at symmetry vanishes. Thus below the Businaro-Gallone point there is no longer a traditional fission saddle point, and fission disappears as a process distinct from evaporation. Thus the mass distribution should show the two evaporation wings extending as far as symmetry where a minimum should be observed. This is illustrated in Fig. 1b.

Such a transition has never been observed, as it requires the measurement of the entire mass distribution from symmetry to the extreme asymmetry of α,p evaporation for a series of systems straddling the Businaro-Gallone point. This measurement is made very difficult by the low yield for symmetric decay of the compound nucleus in this general mass region, and by the need to verify that the fragments were produced by a compound nucleus mechanism.[6]

We have measured[10] complete charge distributions from protons to symmetric splitting for a variety of nuclei and we have observed the Businaro-Gallone transition. Such a transition is inferred from the disappearance of the fission peak in the mass yield as the compound nucleus mass was decreased from ^{148}Eu, ^{102}Rh to ^{83}Kr.

The use of reverse kinematics (projectile heavier than the target) was crucial in performing these measurements. This technique virtually eliminates the problems associated with low cross section measurements due to the presence of light element target contaminants. Furthermore, reverse kinematics provides a large center-of-mass (c.m.) velocity which facilitates the verification of full momentum transfer and allows for easy identification of the fragment's atomic number at the higher lab energies. Finally the high energy solution at forward angles corresponds to very backward angles in ordinary kinematics. This enhances the observation of compound nucleus decay and virtually eliminates any possible deep-inelastic contamination.

The experiments were carried out at the Lawrence Berkeley Laboratory SuperHILAC utilizing beams of 550-Mev ^{74}Ge, 782-MeV ^{93}Nb and 1157-MeV ^{139}La, to bombard targets of 0.54 mg/cm^2 ^{12}C and 1.0 mg/cm^2 ^{9}Be.

The observed laboratory energies represent only the higher energy kinematic solution. In general, the lower solution is not observed because of the energy threshold due to the thickness of our ΔE detectors. Thus the laboratory energy of the upper solution, the measured atomic number (Z), and angle permitted us to verify that the recorded events both originated from a system with full momentum transfer and had a c.m. energy independent of angle. This is shown for two representative elements in Fig. 7.

The mean laboratory energies for each Z-value were converted to velocities with two different assumptions for the relationship between the Z and the mass of the detected fragments. These velocities are then decomposed into two components. One component, along the beam direction, is assigned an arbitrary value; the other component is that required to reconstitute the

original velocity. (For convenience this second component is shown as the c.m. energy in Fig. 7.) In this way, for each laboratory angle we can draw a curve representing the dependence of the c.m. energy upon the source velocity. This procedure is followed for each angle that is smaller than the kinematically allowed maximum angle. The intersection of these lines determines, in a model independent way, both the momentum transfer and the energy in the center of mass. The error bars shown on the lines in Fig. 7 reflect the uncertainty in the mean laboratory energies.

The results from this type of analysis for the $^{93}Nb + ^{12}C$ system are shown in Fig. 8. The upper part of this figure demonstrates that with either mass assumption all of the measured products result from the decay of a system with full momentum transfer. For the other systems studied, the extracted source velocities are also independent of Z within a few percent of the velocity expected for full momentum transfer. The deduced c.m. energies are shown in the lower portion of Fig. 8. These energies are reproduced by a Coulomb calculation for two spheres with a surface separation of 2 fm. This same separation also reproduces the c.m. energies from the ^{74}Ge induced reactions; however a larger separation is required for the ^{139}La data. Both the full momentum transfer and the invariance with angle of the c.m. energies seen above are consistent with compound nucleus decay.

The experimental cross sections for 530-MeV ^{74}Ge, 782-MeV ^{93}Nb and 1157-MeV $^{139}La + ^{9}Be$ systems are shown in Fig. 9. The cross sections are plotted as a function of charge asymmetry ($Z_{asy} = Z_{detected}/Z_{total}$). The lack of enhancement in yield near the target Z supports the compound nucleus origin of the products rather than a deep-inelastic origin. The yield from the $^{74}Ge + ^{9}Be$ system, with a fissility parameter of x = 0.31, decreases steadily as one moves towards symmetry. The yields from the $^{93}Nb + ^{9}Be$ system (x = 0.40) are essentially constant from $Z_{asy} = 0.2$ to 0.4 while the yields from the $^{139}La + ^{9}Be$ system (x = 0.50) show the characteristic fission peak at symmetry. These three systems clearly exhibit the qualitative trends expected from the topological changes in the potential energy surface predicted by the liquid drop model (see Fig. 1).

A quantitative comparison between these data and a compound nucleus calculation based upon the liquid drop model is also shown in Fig. 9. The absolute yields were calculated from the expression

$$\sigma_Z = \pi \lambda^2 \sum_{\ell=0}^{\ell_m} (2\ell + 1) \frac{\Gamma_Z(\ell)}{\Gamma_n + \Gamma_p + \Gamma_\alpha} \tag{7}$$

where $\frac{\Gamma_Z}{\Gamma_n}$ is given by Eq. (1).

The angular distribution expressions given in Ref. 5 were employed to calculate the differential cross section ($d\sigma/d\Omega$). The c.m. angles of the data in Fig. 9 vary as a function of Z. However, the average c.m. angle is approximately 30°, so this angle was chosen for comparison. The agreement in absolute magnitude and in trend between this calculation and the data confirms the compound nuclear origin of these fragments.

In summary, we have shown that fragments with atomic numbers covering the entire range of the mass asymmetry coordinate are produced from the decay of an excited compound nucleus. The observed Z distributions indicate that the topological transition expected at the Businaro-Gallone point does indeed take place in the region of A ~ 100. The exact position of the Businaro-Gallone point and its angular momentum dependence can in principle be established by a systematic study of the Z or A distributions as the fissility parameter x and the rotational parameter y are varied.

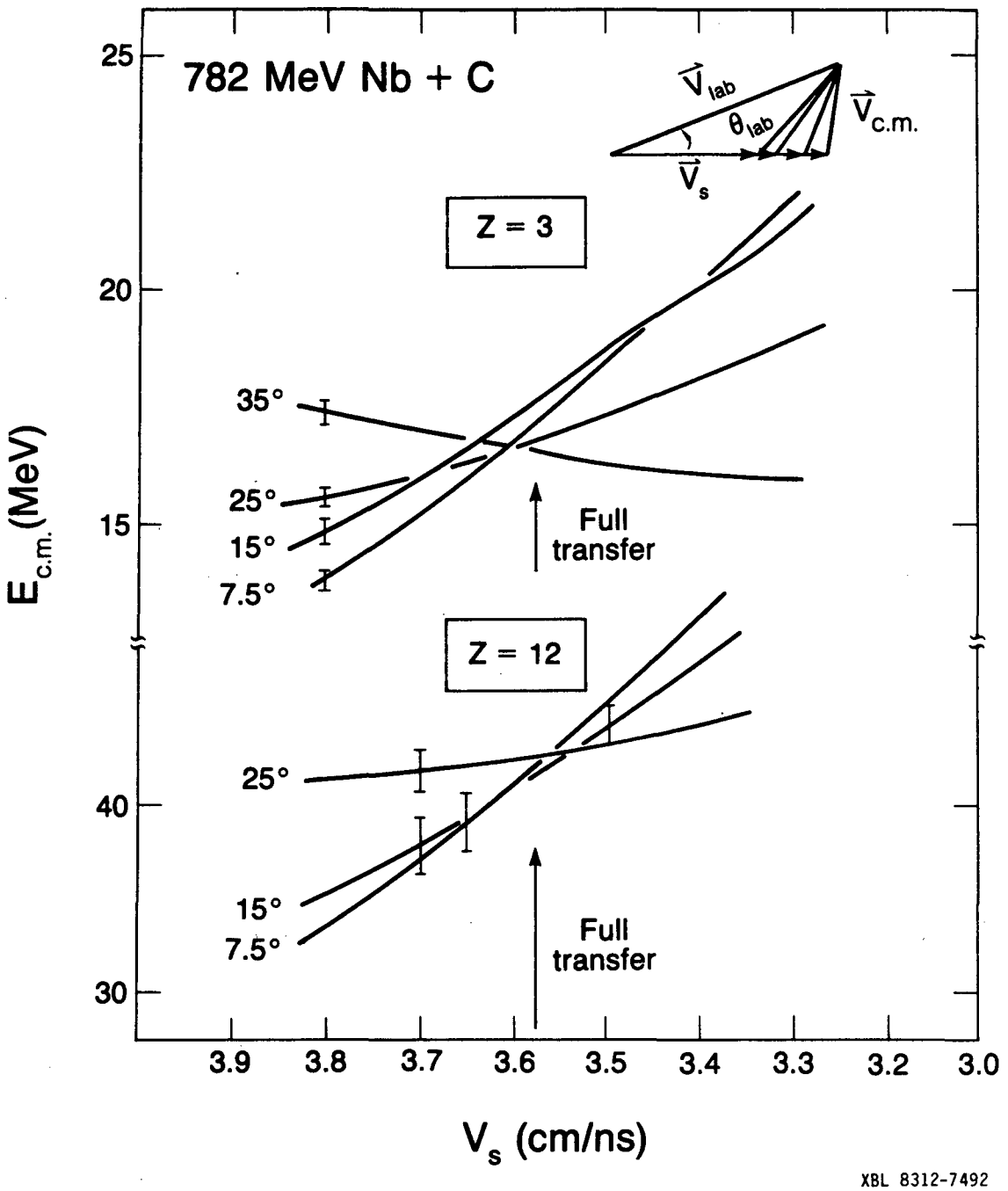

XBL 8312-7492

Fig. 7. The line for each angle gives the locus of solutions for both $E_{c.m.}$ and V_s. The intersection of the various lines fixes these quantities. The velocity corresponding to complete linear momentum transfer is indicated. This figure was drawn assuming that the masses follow the line of β-stability.

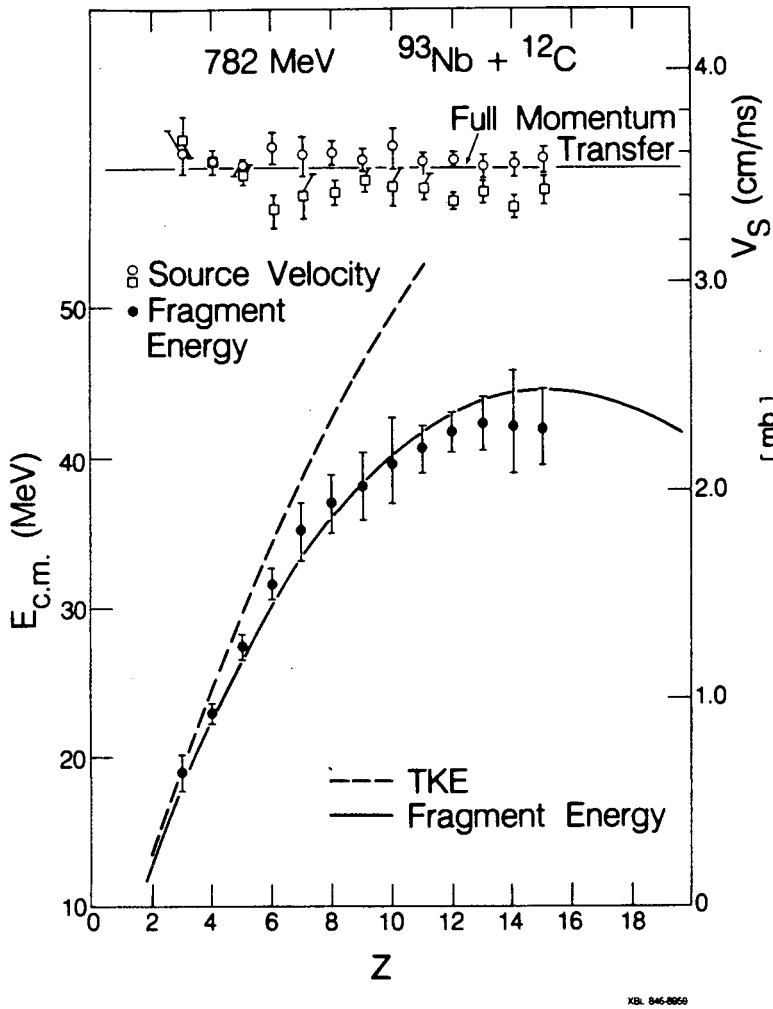

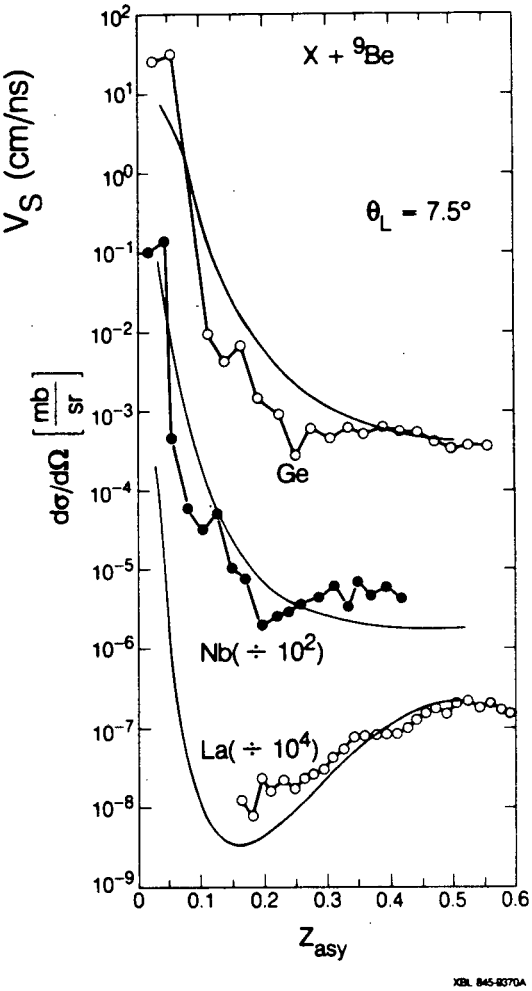

Fig. 8. The deduced c.m. energies (filled) circles) and source velocities (open symbols) for the $^{93}Nb + ^{12}C$ system. Source velocities were determined assuming that the product mass followed the line of β-stability (open circles) or the charge equilibration line (open squares). A Coulomb calculation for two spheres is shown both for the c.m. energy of the light fragment (solid line) and the total kinetic energy (dashed line). The value of the source velocity expected for full momentum transfer is indicated by the horizontal line. The error bars indicate the uncertainty of the intersection point shown in Fig. 7.

Fig. 9. Center-of-mass cross sections for products from the ^{74}Ge, ^{93}Nb and $^{139}La + ^{9}Be$ systems detected at θ_{Lab} = 7.5. The solid line is a liquid drop model calculation of the fragment yield at $\theta_{c.m.}$ = 30. The arrows indicate the entrance channel asymmetry. See text. Data below z_{asy} = 0.15 were not obtained for the La + Be system, due to a limited dynamic range of the telescope.

Having managed to characterise the compound nucleus emission of complex fragments at low energy in satisfactory detail, we now proceed to see what happens when we increase the energy in the region where new mechanisms have been claimed to prevail. At higher energies the use of target-projectile combinations of nearly equal size showed us that, a) complete fusion disappeared; b) the projectile-like fragment appeared to proceed forward with a rather broad distribution of momenta and decayed in some yet unclear way by emitting complex fragments. In order to clean up the picture we decided to use a light target (^{9}Be,Al) and a moderately heavy projectile (Nb) in order to minimize the range of impact parameters and the associated distribution of momentum transfers on one hand and in order to take advantage of the reverse kinematics on the other. Such a decision paid off immediately. As can be seen in fig. 10 for the reaction ^{9}Be + Nb at 25 MeV per nucleon, the energy of the particles as a function of Z is double valued, the two solutions being narrow and well separated. This measurement alone tells us that the complex particles are emitted in a process that is binary with Coulomb-like energies. The two solutions in fact correspond to the double intersection of the laboratory angle with the kinematic circle of the Coulomb velocities. More precisely the emitting source is moving with a velocity that is nearly that of the compound nucleus, and it is formed by fusion of all but 2.5 mass units on the average of the ^{9}Be with the Nb. The same data seen in coincidence in fig. 11 show that indeed the process is binary and that the sum of the fragment charges is nearly constant though smaller than the compound nucleus charge. The missing charge can be neatly explained by sequential evaporation as shown in fig. 12 where the experimental sum of charges is compared with the result of an evaporation code.

The large blob of events at the greatest Z's visible in fig. 10 is the tail end of the evaporation residue which extends as far as the inner side

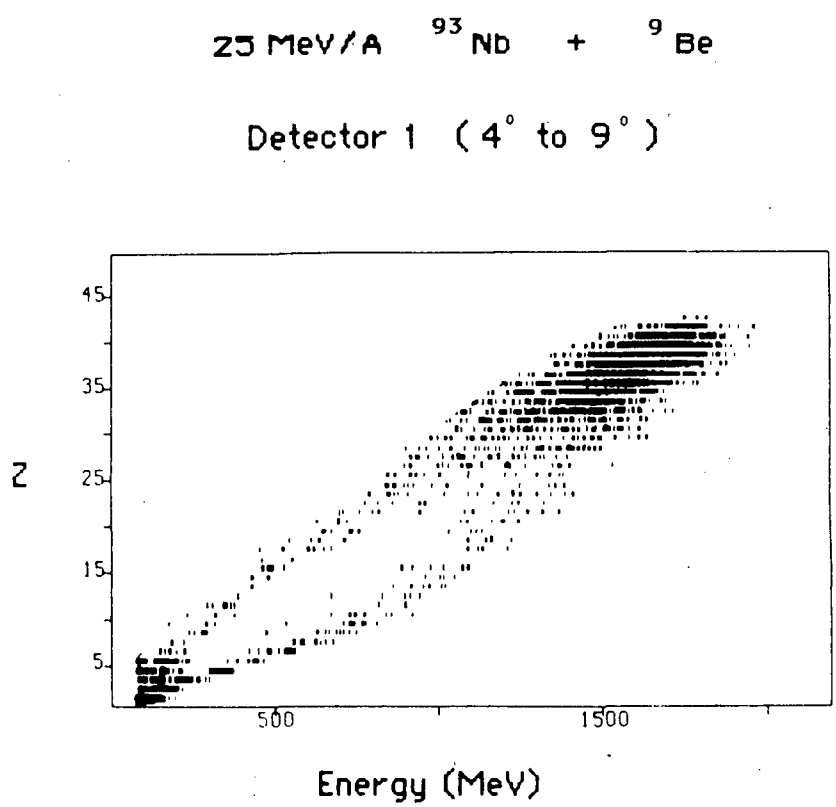

Fig. 10. Singles events in the charge, energy plane for the reaction 25 MeV per nucleon ^{93}Nb + ^{9}Be.

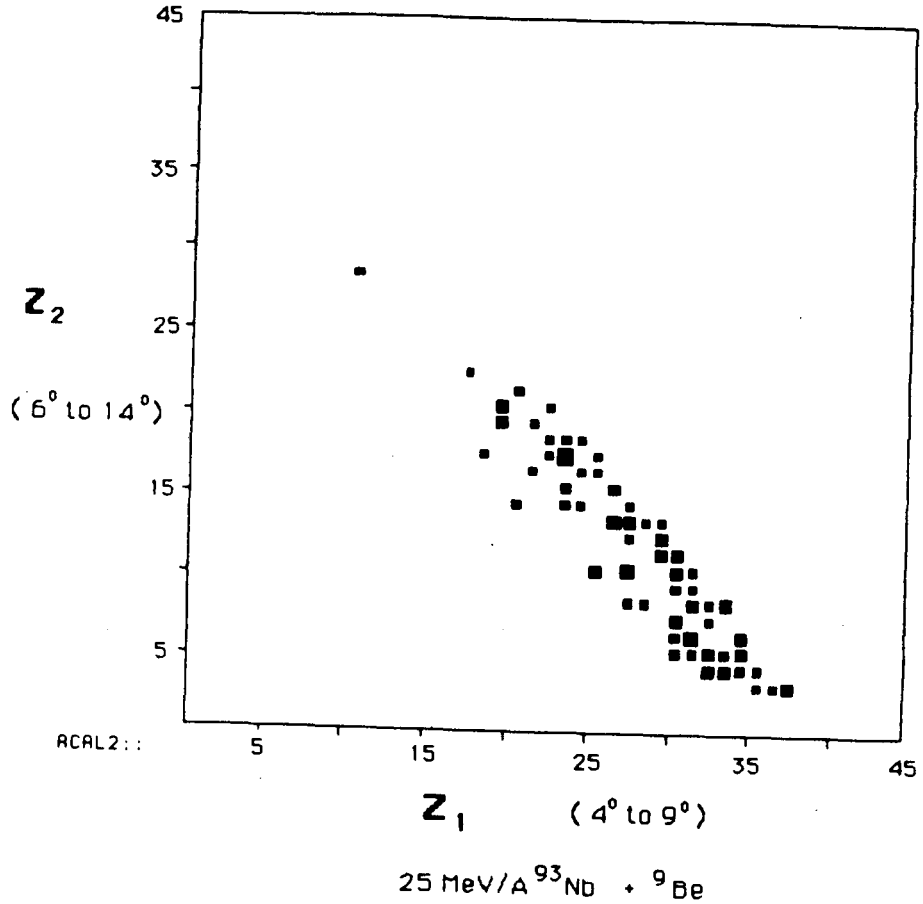

Fig. 11. Z_1, Z_2 coincidences in the same reaction as in Fig. 10.

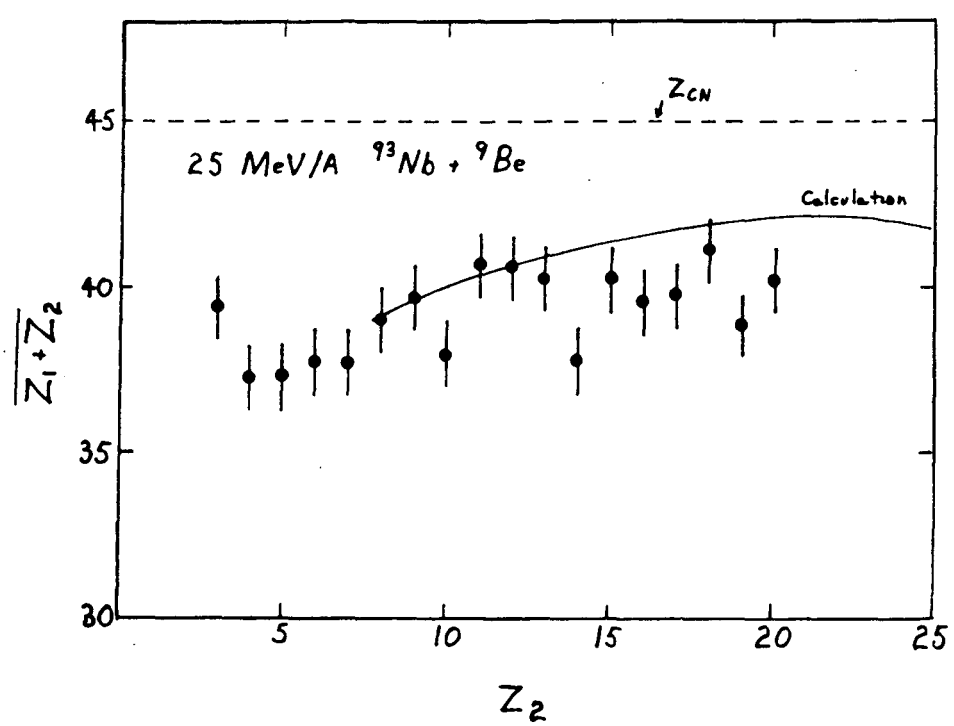

Fig. 12. Mean value of the sum $Z_1 + Z_2$ as a function of Z_2. The solid line is obtained by means of an evaporation code.

of our detector as verified with an evaporation simulation.

Similar results we have obtained up to 40 MeV/A with the ^{9}Be target and with the Al target.

In the course of this work we have learnt of a similar experiment at Ganil in which very similar results have been obtained.[11]

The conclusions that can be drawn from these preliminary data are rather firm. The great majority of the complex fragments produced in these reactions is associated with a binary decay from a source with a large momentum transfer. All the indications point to a compound nucleus formed by the nearly complete fusion of Be and Nb which in turn decays by a binary process to yield complex fragments, much like what we saw at much lower energy.

Mechanisms like cold fragmentation or liquid vapor equilibrium are inherently higher multiplicity processes which are inconsistent with the observed binary decay. Consequently these mechanisms must be ruled out in the energy regime of our investigation and should be looked for at higher energy where, undoubtedly, the complex fragments will be associated with higher multiplicity events.

This work was supported by the Director, Office of Energy Research, Division of Nuclear Physics of the Office of High Energy and Nuclear Physics of the U.S. Department of Energy under Contract DE-AC03-76SF00098.

4. REFERENCES

1. Hyde, E.K., The Nuclear Properties of the Heavy Elements, Vol III: Fission Phenomena, Prentice-Hall, Inc., 1964, Ch. 11 and references therein
2. Poskanzer, A.M., Butler G.W. and Hyde, E.K., Phys. Rev. C3 (1971) 882; ibid C5 (1971) 1795.
3. Aichelin J. and Hüfner, J., Phys. Lett. 136B (1984) 15.
4. See for instance Finn, J.E. et al., Phys. Rev. Lett. 49 (1982) 1321.
5. Moretto, L.G., Nucl. Phys. A247 (1975) 211.
6. Sobotka, L.G., Padgett, M.A., Wozniak, G.J., Guarino, G., Pacheco, A.J., Moretto, L.G., Chan, Y., Stokstad, R.G., Tserruya, I. and Wald, S., Phys. Rev. Lett. 51 (1983) 2187.
7. Westfall, G.D. et al., Phys. Rev. C17 (1978) 1368.
8. Green, R. and Korteling, R., Phys. Rev. C22 (1980) 1594.
9. Sierk, A.J., preprint LA-UR85-1660, 1985.
10. Sobotka, L.G., McMahan, M.A., McDonald, R.J., Signarbieux, C., Wozniak, G.J., Padgett, M.L., Gu, J.H., Liu, Z.H., Yao Z.O. and L.G. Moretto, Phys. Rev. Lett.
11. Mittig W. et al., Phys. Lett. 154B (1985) 259.

This report was done with support from the Department of Energy. Any conclusions or opinions expressed in this report represent solely those of the author(s) and not necessarily those of The Regents of the University of California, the Lawrence Berkeley Laboratory or the Department of Energy.

Reference to a company or product name does not imply approval or recommendation of the product by the University of California or the U.S. Department of Energy to the exclusion of others that may be suitable.

LAWRENCE BERKELEY LABORATORY
TECHNICAL INFORMATION DEPARTMENT
UNIVERSITY OF CALIFORNIA
BERKELEY, CALIFORNIA 94720